



HAL
open science

How close are shell models to the 3D Navier–Stokes equations?

Dario Vincenzi, John D Gibbon

► **To cite this version:**

Dario Vincenzi, John D Gibbon. How close are shell models to the 3D Navier–Stokes equations?. Nonlinearity, 2021, 34 (8), pp.5821-5843. 10.1088/1361-6544/abe096 . hal-03453319

HAL Id: hal-03453319

<https://hal.science/hal-03453319>

Submitted on 28 Nov 2021

HAL is a multi-disciplinary open access archive for the deposit and dissemination of scientific research documents, whether they are published or not. The documents may come from teaching and research institutions in France or abroad, or from public or private research centers.

L'archive ouverte pluridisciplinaire **HAL**, est destinée au dépôt et à la diffusion de documents scientifiques de niveau recherche, publiés ou non, émanant des établissements d'enseignement et de recherche français ou étrangers, des laboratoires publics ou privés.

How close are shell models to the 3D Navier–Stokes equations?

Dario Vincenzi^{1‡} and John D Gibbon²

¹ Université Côte d’Azur, CNRS, LJAD, 06100 Nice, France

² Department of Mathematics, Imperial College London, London SW7 2AZ, UK

E-mail: dario.vincenzi@univ-cotedazur.fr, j.d.gibbon@imperial.ac.uk

Abstract. Shell models have found wide application in the study of hydrodynamic turbulence because they are easily solved numerically even at very large Reynolds numbers. Although bereft of spatial variation, they accurately reproduce the main statistical properties of fully-developed homogeneous and isotropic turbulence. Moreover, they enjoy regularity properties which still remain open for the three-dimensional (3D) Navier–Stokes equations (NSEs). The goal of this study is to make a rigorous comparison between shell models and the NSEs. It turns out that only the estimate of the mean energy dissipation rate is the same in both systems. The estimates of the velocity and its higher-order derivatives display a weaker Reynolds number dependence for shell models than for the 3D NSEs. Indeed, the velocity-derivative estimates for shell models are found to be equivalent to those corresponding to a velocity gradient averaged version of the 3D Navier–Stokes equations (VGA-NSEs), while the velocity estimates are even milder. Numerical simulations over a wide range of Reynolds numbers confirm the estimates for shell models.

AMS classification scheme numbers: 37N10, 76F02.

Submitted to: *Nonlinearity*

Keywords: Turbulence, Shell models, High-order moments of the velocity derivatives

1. Introduction

Three-dimensional (3D) incompressible turbulent flows are characterized by a cascade of kinetic energy from the length scales at which the flow is generated to the scales at which viscous dissipation becomes predominant [1–4]. Kinetic energy is usually injected at large scale by a body forcing or the boundary conditions, and, on average, it is transferred at a constant rate to smaller scales by nonlinear interactions between the Fourier modes of the velocity. The energy is strongly dissipated when the viscous-dissipation range is reached. The range between the forcing and viscous scales is known as inertial range and is characterized by a kinetic-energy spectrum that, up to intermittency corrections, behaves as $E(k) \sim k^{-5/3}$, where k is the wavenumber.

‡ Also Associate, International Centre for Theoretical Sciences, Tata Institute of Fundamental Research, Bangalore 560089, India.

When the viscosity tends to zero while the scale and the magnitude of the large-scale velocity remain fixed, the energy dissipation rate has a nonzero limit [5, 6], which is known as the ‘dissipative anomaly’.

A mathematically rigorous description of the generation of small scales in turbulent 3D Navier–Stokes flows can be achieved by considering the L^{2m} -norms of the velocity derivatives for weak solutions of the Navier–Stokes equations (NSEs) [7–10]. Given a velocity field \mathbf{u} over a periodic cube $\mathcal{V} = [0, L]^3$, volume integrals and norms can be defined as

$$H_{n,m}(t) = \int_{\mathcal{V}} |\nabla^n \mathbf{u}|^{2m} dV. \quad (1)$$

The well known scaling property of the NSEs $\mathbf{u}(\mathbf{x}, t) \rightarrow \mu^{-1} \mathbf{u}(\mathbf{x}/\mu, t/\mu^2)$ suggests the definition of a doubly-labelled set of dimensionless, invariant quantities [10]

$$F_{n,m}(t) = \nu^{-1} L^{1/\alpha_{n,m}} H_{n,m}^{1/2m}, \quad (2)$$

for $0 \leq n < \infty$ and $1 \leq m \leq \infty$, where ν is the kinematic viscosity and

$$\alpha_{n,m} = \frac{2m}{2m(n+1) - 3}. \quad (3)$$

It was shown in [9, 10] that for $1 \leq n < \infty$ and $1 \leq m \leq \infty$, together with $n = 0$ for $3 < m \leq \infty$

$$\langle F_{n,m}^{\alpha_{n,m}} \rangle_T \leq c_{n,m} Re^3 + O(T^{-1}) \quad (Re \gg 1), \quad (4)$$

where Re is the Reynolds number and the time average up to time $T > 0$ is defined by

$$\langle \cdot \rangle_T = T^{-1} \int_0^T \cdot dt. \quad (5)$$

Moreover, the set of estimates in (4) encompasses all the known a priori bounds for weak solutions of the 3D NSEs equations and shows how these bounds arise naturally from scale invariance [9, 10]. In those references it has been shown that a hierarchy of spatially averaged length scales $\ell_{n,m}(t)$ can be constructed from the $F_{n,m}$ in the following manner :

$$(L\ell_{n,m}^{-1})^{n+1} := F_{n,m}. \quad (6)$$

Higher values of n allow the detection of smaller scales, while higher values of m account for stronger deviations from the mean. Using (4) and (6), followed by a Hölder inequality, one finds that

$$\langle L\ell_{n,m}^{-1} \rangle_T \leq c_{n,m} Re^{\frac{3}{(n+1)\alpha_{n,m}}} \quad (Re \gg 1). \quad (7)$$

As noted in [9], while the estimate for the first in the hierarchy is $Re^{3/4}$ and is consistent with the inverse Kolmogorov length, the limit as $n, m \rightarrow \infty$ is finite and is consistent with the fact that viscosity ultimately dissipates the cascade of energy§.

§ Strictly speaking there is a limit to the value of Re beyond which kinetic scales are reached and the NSEs become invalid.

The Re dependence of the moments of $\nabla\mathbf{u}$ has been studied within the multifractal formalism [1, 11, 12] and in numerical simulations of both the 3D NSE [13] and the Burgers equation [14]. The calculation of $H_{n,m}$ for high Re and large values of n and m nonetheless requires large numerical simulations (see [15] for the $n = 1$ case). At high Re , indeed, the injection and viscous-dissipation scales are widely separated, and the cascade process activates a wide range of length scales: an empirical argument due to Landau and Lifschitz [16] indicates that the number of degrees of freedom of a turbulent velocity field grows as $Re^{9/4}$ (see also [1]). For this reason, the direct numerical simulation of high- Re flows have remained a great challenge [17–21]. In order to study the properties of fully developed turbulence, simplified models have thus been introduced that retain some of the properties of the NSEs but are much more tractable both theoretically and numerically. Among these, shell models of the energy cascade have played a major role [1, 22–24]. They consist of a system of ordinary differential equations for a set of complex scalar variables which can be regarded loosely as the amplitudes of the Fourier components of the velocity field. The structure of the equations mimics that of the NSEs in Fourier space. The nonlinear part has a form that recalls the vortex-stretching term, but the interactions between the velocity variables are local. A linear small-scale dissipation and generally a forcing are also included. Because of their scalar nature, shell models are unable to provide information on the spatial structure of the velocity field. However, they successfully reproduce the statistical properties of space-averaged quantities, such as the kinetic-energy spectrum, the velocity structure functions or the viscous-dissipation rate in isotropic turbulence. From a mathematical point of view, stronger results have been proved for shell models than for the 3D NSEs: for instance, the global regularity of strong solutions and the existence of a finite-dimensional inertial manifold [25, 26] (see [27] for analogous results on stochastic shell models).

Questions still remain, however, over how close the mathematical results of shell-models are to those for the NSEs. Shell-models are bereft of spatial variation while the behaviour of solutions of the NSEs equations differ widely depending upon their dimension. Indeed, although the notion of velocity gradient as a spatio-temporal field in shell models is not available, it is easy to define the analogue of the volume integral of powers of the velocity derivatives. For instance, the shell-model analogues of enstrophy and helicity have been studied extensively [22–24]. Nevertheless, it is not clear where the exact correspondence lies. The goal of this paper is to investigate the analogue of $H_{n,m}$ for shell models, both mathematically and numerically, in relation to the NSEs equations to see if there is a consistent correspondence between the two.

The paper is organized in the following steps. Section 2 introduces the shell model and the mathematical framework. We consider the ‘Sabra’ model [28], but the results are general and, in particular, also hold for the GOY model [29, 30], the only difference being in the constants that appear in the estimates.

The starting point of our study is a bound for the mean energy-dissipation rate, which corresponds to the $m = n = 1$ case. This is obtained in section 3 by adapting to

shell models the methods used by Doering and Foias [31] for the NSEs (see also [32,33] for the application of the same methods to magnetohydrodynamics and binary mixtures). The estimate for the dissipation rate coincide, as expected, with that for the 3D NSEs.

In sections 4.1 and 4.2, we keep $m = 1$ but move to general n , i.e. we study $H_n \equiv H_{n,1}$, the analogue of the L^2 -norm of the n -th order derivative of the velocity. We first prove two differential relations connecting H_n and H_{n+1} , in the spirit of the “ladder” relations available for the NSEs [34,35]. Following the strategy applied in [35–37], we then use these relations together with the bound for the energy dissipation rate to prove the existence of absorbing balls for all H_n and to estimate the time average $\left\langle H_n^{\frac{2}{n+1}} \right\rangle_T$ in terms of Re . This latter result is the counterpart of a bound proved by Foias, Guillopé and Temam [38] for weak solutions of the 3D NSEs. It is further extended to general n and m in section 4.3, where it is shown that, in terms of the $\alpha_{n,m}$ defined above in (3) and (4), the shell-model equivalent is

$$\alpha_{n,m} = \frac{4}{n+1}, \quad (8)$$

which is independent of m .

The form of these bounds and, in particular, their insensitivity to m , raise the question of how close these results are to the NSEs in any dimension. Comparing (8) with (3), we find that $\alpha_{n,m}$ is greater for shell models than for the 3D NSEs for all $n > 1$ and $1 \leq m \leq 0$. Therefore, the Re dependence of the high-order velocity derivatives differs in the two systems and, in shell models, is significantly weaker. It is indeed discovered in section 5 that, as far as the velocity-derivative estimates are concerned, the real PDE-equivalent of the shell models considered here is not the full 3D NSEs themselves but a version of these that we have called the ‘velocity gradient averaged Navier–Stokes equations’ (VGA-NSEs). While less specific in its definition as intermittency in multi-fractal theories [1], intermittent events in solutions of the NSEs have the property that excursions in $\nabla \mathbf{u}$ depart strongly from its average $\|\nabla \mathbf{u}\|_2$, thereby implying that for very short periods of time

$$L^{3/2} \frac{\|\nabla \mathbf{u}\|_\infty}{\|\nabla \mathbf{u}\|_2} \gg 1, \quad (9)$$

whereas making the approximation

$$L^{3/2} \frac{\|\nabla \mathbf{u}\|_\infty}{\|\nabla \mathbf{u}\|_2} = 1, \quad (10)$$

has the effect of suppressing strong events in $\nabla \mathbf{u}$. The VGA-NSEs are obtained by using (10) in the differential inequalities for the NSEs. In fact, it can be thought of in the following way: a Gagliardo–Nirenberg inequality shows that

$$\frac{\|\nabla \mathbf{u}\|_\infty}{\|\nabla \mathbf{u}\|_2} \leq c_n \kappa_n^{3/2}, \quad \kappa_n = \left(\frac{\|\nabla^{n+1} \mathbf{u}\|_2}{\|\nabla \mathbf{u}\|_2} \right)^{1/n}. \quad (11)$$

The wave-number $\kappa_n(t)$ behaves as a higher moment of the enstrophy spectrum and has a lower bound expressed as $L^{-1} \leq \kappa_n(t)$. (10) occurs when one uses only the minimum

of the right-hand side of the inequality in (11). One of the main results of this paper is that for all $n \geq 1$ and $1 \leq m \leq \infty$, the bounds and the exponents in the various bounded time-averages of VGA-NSEs and the shell models are equivalent.

The velocity estimates for the shell models are even milder than those for the VGA-NSEs. Indeed, it is shown that for the VGA-NSEs

$$\langle \|\mathbf{u}\|_m^2 \rangle_T \leq c_m \nu^2 L^{-\frac{2m-3}{m}} Re^3 \quad (m \geq 1), \quad (12)$$

whereas the shell-model analogues of $\langle \|\mathbf{u}\|_m^2 \rangle_T$ scale as Re^2 .

Finally, section 6 concludes the paper by summarizing the estimates for shell models and comparing them with numerical simulations of the ‘Sabra’ model over a wide range of values of Re .

2. The ‘Sabra’ shell model

Shell models of turbulence describe the velocity field by means of a sequence of complex variables u_j , $j = 1, 2, 3, \dots$, which represent its Fourier components. In the ‘Sabra’ model [28], the variables u_j satisfy the following equations:

$$\dot{u}_j = i(ak_{j+1}u_{j+1}^*u_{j+2} + bk_ju_{j+1}u_{j-1}^* - ck_{j-1}u_{j-1}u_{j-2}) - \nu k_j^2 u_j + f_j, \quad (13)$$

where $k_j = k_0 \lambda^j$ ($k_0 > 0$, $\lambda > 1$) are logarithmically-spaced wave numbers, ν is the kinematic viscosity, and the f_j are complex and represent the Fourier amplitudes of the forcing. The ‘boundary conditions’ for the velocity variables are $u_0 = u_{-1} = 0$, while k_0^{-1} plays the role of the largest spatial scale in the system. The coefficients a , b , c are real and satisfy

$$a + b + c = 0. \quad (14)$$

This condition ensures that the kinetic energy,

$$E = \sum_{j=1}^{\infty} |u_j|^2, \quad (15)$$

is conserved when $\nu = 0$ and $f_j = 0$ for all j . In the inviscid, unforced case and under condition (14), the shell model also possesses a second quadratic invariant, which for suitable values of a , b , c can be interpreted as either a generalized helicity or a generalized enstrophy [22]. The parameters of the shell model can also be tuned so as to generate an inverse cascade of energy from small to large scales, as in two-dimensional turbulence [39]. In the following, however, we shall not impose any additional constraint on a , b , c other than (14).

Various forcings have been considered in the literature, such as those that act only on few low- j shells and mimic the injection of energy at large scales [28, 30], those that impose a constant energy input [40], or those with a power-law ‘spectrum’ [41, 42]. We consider a constant-in-time deterministic forcing, but the results are easily generalized

to time-dependent f_j . Following [31], we define the forcing in a way as to isolate its magnitude from its shape. We take

$$f_j = \mathcal{F} \phi_{j-j_f}, \quad (16)$$

where \mathcal{F} is a complex constant, $j_f \geq 1$, and the shape function ϕ_p is such that $\phi_p = 0$ if $p < 0$. Thus, $k_f = k_0 \lambda^{j_f}$ is the characteristic wavenumber of the forcing. We also assume

$$\sum_{p=0}^{\infty} |\phi_p|^2 < \infty \quad (17)$$

and

$$\sum_{p=0}^{\infty} \lambda^{-2p} |\phi_p|^2 = 1. \quad (18)$$

The assumption in (17) means that the ‘energy’ of the forcing is finite, while (18) is a normalization condition on the shape function. In sections 4 and 5, we shall further require that the forcing has a maximum wavenumber k_{\max} .

Under assumption (17), it was shown in [25] that if the energy E is bounded at time $t = 0$, then it stays bounded at any later time. This allows us to define the root mean square velocity

$$U = \langle E \rangle_T^{1/2}, \quad (19)$$

where the time average up to time T has been introduced in (5). In addition, the time-averaged dissipation rate

$$\epsilon = \nu \left\langle \sum_{j=1}^{\infty} k_j^2 |u_j|^2 \right\rangle_T \quad (20)$$

is also bounded for all $T > 0$ [25]. By using U , k_f , and $|\mathcal{F}|$, we can then define the Reynolds and Grashof numbers as

$$Re = \frac{U}{\nu k_f} \quad \text{and} \quad Gr = \frac{|\mathcal{F}|}{\nu^2 k_f^3}, \quad (21)$$

respectively. The latter is a dimensionless measure of the forcing, while the former quantifies the response of the system.

Finally, we note that it is possible to introduce a suitable functional setting for the study of (13), in which a solution $\mathbf{u} = (u_1, u_2 \dots)$ is regarded as an element of the sequences space ℓ^2 over the field of complex numbers, with scalar product $(\mathbf{u}, \mathbf{v}) = \sum_{j=1}^{\infty} u_j v_j^*$ for any $\mathbf{u}, \mathbf{v} \in \ell^2$ [25]. Here, however, we follow the physical notation and work with the variables u_j directly.

3. The time-averaged energy dissipation rate

An estimate of the time-averaged energy dissipation rate ϵ , defined in (20), is an essential element of the present study as results on the high-order derivatives of the velocity are based on this. It was once conventional to write estimates for ϵ in terms of the Grashof number Gr until Doering and Foias [31] introduced a method that converted these into estimates in terms of the Reynolds number Re , which is much more useful for comparison with other theories of turbulence. The methods used here are adapted from Doering and Foias [31].

Let us first introduce the constants that will appear in the estimate for ϵ :

$$A = |a|\lambda + |b| + |a + b|\lambda^{-1}, \quad B_\gamma = \sup_{p \geq 0} \lambda^{-(2\gamma-1)p} |\phi_p|, \quad C_\gamma = \sum_{p=0}^{\infty} \lambda^{2\gamma p} |\phi_p|^2. \quad (22)$$

A is a function of the parameters of the shell model, while B_γ and C_γ are fixed by the shape of the forcing. The exponent γ is a real number and must be such that B_γ and C_γ are finite; in particular, the normalization condition in (18) implies $C_{-1} = 1$. It is important to stress that B_γ and C_γ depend neither on the amplitude nor on the characteristic wavenumber of the forcing. We shall also make use of the following result:

Lemma 1. *For any $\gamma \in \mathbb{R}$ such that C_γ is finite,*

$$\sum_{j=1}^{\infty} k_j^{2\gamma} |f_j|^2 = C_\gamma k_f^{2\gamma} |\mathcal{F}|^2. \quad (23)$$

Proof. By using the definition of the forcing in (16) and rearranging the terms in the sum, we obtain:

$$\sum_{j=1}^{\infty} k_j^{2\gamma} |f_j|^2 = |\mathcal{F}|^2 \sum_{j=j_f}^{\infty} k_j^{2\gamma} |\phi_{j-j_f}|^2 = |\mathcal{F}|^2 \sum_{p=0}^{\infty} k_{p+j_f}^{2\gamma} |\phi_p|^2 \quad (24)$$

$$= |\mathcal{F}|^2 \sum_{p=0}^{\infty} k_0^{2\gamma} \lambda^{2\gamma(p+j_f)} |\phi_p|^2 = |\mathcal{F}|^2 (k_0 \lambda^{j_f})^{2\gamma} \sum_{p=0}^{\infty} \lambda^{2\gamma p} |\phi_p|^2. \quad (25)$$

Replacing the definitions of k_f and C_γ in (25) yields the result. \square

As discussed above at the beginning of this section we now use the method of Doering and Foias [31] to estimate the time-averaged dissipation rate ϵ .

Theorem 1. *Let the forcing (f_1, f_2, \dots) be as in Sect. 2 and the initial energy $E(0)$ be bounded. Then the time-averaged energy dissipation rate satisfies*

$$\epsilon \leq \nu^3 k_f^4 (c_1 Re^2 + c_2 Re^3) + O(T^{-1}), \quad (26)$$

where the constants

$$c_1 = \frac{\sqrt{C_0 C_{2(1-\gamma)}}}{C_{-\gamma}}, \quad c_2 = A \frac{\sqrt{C_0} B_\gamma}{C_{-\gamma}}, \quad (27)$$

depend on the parameters a, b, λ of the shell model and on the shape of the forcing (ϕ_1, ϕ_2, \dots) , but are uniform in $\nu, k_0, k_f, |\mathcal{F}|$. The value of $\gamma \in \mathbb{R}$ may be chosen in a

way as to minimize c_1 and c_2 , but it must nonetheless be such that $C_{-\gamma}$, $C_{2(1-\gamma)}$, B_γ are finite.

Remark 1. The switch from Re^2 to Re^3 behaviour in (26) is observed in the numerical computations displayed in Fig. 1.

Proof. We begin by writing the evolution equation for the energy. Towards this end, we multiply (13) by u_j^* and the complex conjugate of (13) by u_j . We then add the two resulting equations and sum over j :

$$\frac{dE}{dt} = -2\nu \sum_{j=1}^{\infty} k_j^2 |u_j|^2 + \sum_{j=1}^{\infty} (f_j u_j^* + f_j^* u_j). \quad (28)$$

By integrating over time and using the Cauchy–Schwarz inequality twice on the last term, we obtain:

$$E(T) + 2\nu \int_0^T \left(\sum_{j=1}^{\infty} k_j^2 |u_j(t)|^2 \right) dt \leq E(0) + 2\sqrt{C_0} U |\mathcal{F}| T, \quad (29)$$

whence

$$\epsilon \leq \sqrt{C_0} U |\mathcal{F}| + \frac{E(0)}{2T}. \quad (30)$$

To express this bound in terms of Re , we need to estimate $|\mathcal{F}|$ in terms of U and k_f . We multiply (13) by $k_j^{-2\gamma} f_j^*$, sum over j , and average over time:

$$\begin{aligned} \left\langle \sum_{j=1}^{\infty} k_j^{-2\gamma} f_j^* \dot{u}_j \right\rangle_T &= \sum_{j=1}^{\infty} k_j^{-2\gamma} |f_j|^2 - \left\langle \nu \sum_{j=1}^{\infty} k_j^{2-2\gamma} u_j f_j^* \right\rangle_T \\ &\quad + \left\langle i \sum_{j=1}^{\infty} k_j^{-2\gamma} f_j^* (a k_{j+1} u_{j+1}^* u_{j+2} + b k_j u_{j+1} u_{j-1}^* - c k_{j-1} u_{j-1} u_{j-2}) \right\rangle_T. \end{aligned} \quad (31)$$

From (28), it is easy to see that $E(t)$ is bounded by a time-independent constant [25]. This follows from using $k_j < k_1$ for all $j > 1$ in the viscous term, the Cauchy–Schwarz inequality on the forcing term, and then Gronwall’s inequality. As a consequence, the left-hand side of (31) is $O(T^{-1})$.

The first term on the right-hand side is calculated from Lemma 1 as:

$$\sum_{j=1}^{\infty} k_j^{-2\gamma} |f_j|^2 = C_{-\gamma} k_f^{-2\gamma} |\mathcal{F}|^2. \quad (32)$$

The second term is estimated by using the Cauchy–Schwarz inequality:

$$\left| \left\langle \nu \sum_{j=1}^{\infty} (k_j^{2-2\gamma} f_j^*) u_j \right\rangle_T \right| \leq \sqrt{C_{2-2\gamma}} \nu U k_f^{2-2\gamma} |\mathcal{F}|. \quad (33)$$

We estimate the third term by moving the forcing out of the sum and using again the Cauchy–Schwarz inequality :

$$\begin{aligned}
& \left| \left\langle i \sum_{j=1}^{\infty} k_j^{-2\gamma} f_j^* (ak_{j+1}u_{j+1}^*u_{j+2} + bk_ju_{j+1}u_{j-1}^* - ck_{j-1}u_{j-1}u_{j-2}) \right\rangle_T \right| \\
& \leq k_f^{-2\gamma+1} |\mathcal{F}| \left| \left\langle \sum_{j=1}^{\infty} \lambda^{-(j-j_f)(2\gamma-1)} \phi_{j-j_f} (a\lambda u_{j+1}^*u_{j+2} \right. \right. \\
& \qquad \qquad \qquad \left. \left. + bu_{j+1}u_{j-1}^* + (a+b)\lambda^{-1}u_{j-1}u_{j-2}) \right\rangle_T \right| \\
& \leq AB_\gamma U^2 k_f^{-2\gamma+1} |\mathcal{F}|. \tag{34}
\end{aligned}$$

We now combine (32) with (33) and (34) and find :

$$|\mathcal{F}| \leq \frac{\sqrt{C_{2-2\gamma}}}{C_{-\gamma}} \nu U k_f^2 + A \frac{B_\gamma}{C_{-\gamma}} U^2 k_f + O(T^{-1}). \tag{35}$$

Inserting (35) into (30) and rearranging finally yields the estimate for ϵ . \square

The implications of (26) for turbulent flows have been discussed thoroughly in [31] within the context of the 3D NSEs (see also [43]). Here we briefly mention the shell-model counterpart of the main points :

- (i) The bound on ϵ can be rewritten as

$$\frac{\epsilon}{U^3 k_f} \leq \frac{c_1}{Re} + c_2 + O(T^{-1}). \tag{36}$$

Thus, in the high- Re limit the saturation of the bound recovers the empirical prediction $\epsilon \sim U^3 k_f$ [1].

- (ii) The estimate of ϵ can be converted into bounds for the Kolmogorov dissipation wavenumber $k_\eta = (\epsilon/\nu^3)^{1/4}$, the Taylor microscale $k_T = (\epsilon/\nu U^2)^{1/2}$, and the Taylor-microscale Reynolds number, $Re_\lambda = U/\nu k_T$. The saturation of these bounds for $Re \rightarrow \infty$ is consistent with the empirical predictions $k_\eta \sim Re^{3/4}$, $k_T \sim Re^{1/2}$, $Re_\lambda \sim Re^{1/2}$ for 3D homogeneous and isotropic turbulence [1].
- (iii) A lower bound for the time-averaged dissipation rate can also be derived by using the shell-model version of the Poincaré inequality :

$$\epsilon \geq \nu k_1^2 \left\langle \sum_{j=1}^{\infty} |u_j|^2 \right\rangle_T = \nu k_1^2 U^2, \tag{37}$$

where we have used $k_1 > k_j$ for all $j > 1$. The latter bound can be rewritten as

$$\frac{\epsilon}{U^3 k_f} \geq \left(\frac{k_1}{k_f} \right)^2 Re^{-1}. \tag{38}$$

Therefore, the small- Re scaling in (36) is sharp. Moreover, if we take $j_f = 1$ and $\phi_p = \delta_{p,0}$, then $k_f = k_1$ and $c_1 = 1$. As a consequence, the upper and lower bounds on ϵ coincide for $Re \rightarrow 0$, i.e. ϵ behaves as $\epsilon/U^3 k_f = Re^{-1}$. This means that the lower bound on ϵ is also optimal.

(iv) Dividing (35) by $\nu^2 k_f^3$ yields:

$$Gr \leq c'_1 Re + c'_2 Re^2 \quad (39)$$

with $c'_1 = c_1/\sqrt{C_0}$ and $c'_2 = c_2/\sqrt{C_0}$. This bound establishes a relation between the forcing (represented by Gr) and the response of the system (represented by Re).

As mentioned earlier, the proof of Theorem 1 parallels that of Doering and Foias [31] for the NSEs. By using the same approach, it is possible to obtain estimates of ϵ in terms of Gr analogous to those available for the NSEs. It can indeed be shown that for $Gr \rightarrow 0$ the lower and upper bounds on ϵ coincide, and hence the time-averaged dissipation rate behaves as $\epsilon = \nu^3 k_f^4 Gr^2$, while for $Gr \rightarrow \infty$ it satisfies the lower bound $\epsilon \geq c_3 \nu^3 k_1^2 k_f^2 Gr$, where the constant c_3 is uniform in ν , k_0 , $|\mathcal{F}|$, and k_f .

4. High-order velocity derivatives

To investigate higher-order derivatives of the velocity, we now consider the sequence of infinite sums

$$H_n = \sum_{j=1}^{\infty} k_j^{2n} |u_j|^2, \quad n \geq 0, \quad (40)$$

which represent the shell-model analogues of the L^2 -norms $\|\nabla^n \mathbf{u}\|_{L^2}^2$. Note that H_0 is the energy E , while the time average of H_1 is proportional to ϵ :

$$\epsilon = \nu \langle H_1 \rangle_T. \quad (41)$$

We also denote the equivalent sums for the forcing variables as

$$\Phi_n = \sum_{j=1}^{\infty} k_j^{2n} |f_j|^2, \quad n \geq 0. \quad (42)$$

Recall from Lemma 1 that $\Phi_n = C_n k_f^{2n} |\mathcal{F}|^2$.

4.1. Ladder inequalities and absorbing balls for H_n

The following theorem shows that there exist two ladders of differential inequalities that connect H_n and H_{n+1} and reproduce the analogous ladder inequalities for the NSEs [34, 35].

Theorem 2. *Let $n \geq 0$ and assume that the forcing (f_1, f_2, \dots) is such that $\Phi_n < \infty$. Then H_n satisfies*

$$\frac{1}{2} \dot{H}_n \leq -\nu H_{n+1} + c_n H_n \sup_{j \geq 1} k_j |u_j| + H_n^{\frac{1}{2}} \Phi_n^{\frac{1}{2}} \quad (43a)$$

and

$$\frac{1}{2} \dot{H}_n \leq -\frac{\nu}{2} H_{n+1} + \frac{d_n}{\nu} H_n \sup_{j \geq 1} |u_j|^2 + H_n^{\frac{1}{2}} \Phi_n^{\frac{1}{2}} \quad (43b)$$

with

$$c_n = \lambda^{-n+1} (|a|\lambda^{-2n} + |b| + |a + b|\lambda^{2n}), \quad d_n = \frac{c_n^2}{2\lambda^4}. \quad (44)$$

Proof. We multiply (13) by $k_j^{2n}u_j^*$ and the complex conjugate of (13) by $k_j^{2n}u_j$. We then sum to obtain

$$\begin{aligned} \dot{H}_n &= -2\nu H_{n+1} \\ &+ \sum_{j=1}^{\infty} k_j^{2n} [iu_j^*(ak_{j+1}u_{j+1}^*u_{j+2} + bk_ju_{j+1}u_{j-1}^* - ck_{j-1}u_{j-1}u_{j-2} + f_j) + \text{c.c.}] , \end{aligned} \quad (45)$$

where ‘c.c.’ stands for ‘complex conjugate’. The forcing term is estimated by using the Cauchy–Schwarz inequality :

$$\left| \sum_{j=1}^{\infty} k_j^{2n} u_j^* f_j \right| = \left| \sum_{j=1}^{\infty} (k_j^n u_j^*) (k_j^n f_j) \right| \leq H_n^{\frac{1}{2}} \Phi_n^{\frac{1}{2}} . \quad (46)$$

Consider then the nonlinear term with coefficient a . We have

$$\left| a \sum_{n=1}^{\infty} k_j^{2n} k_{j+1} u_j^* u_{j+1}^* u_{j+2} \right| \leq |a| \lambda^{-3n+1} \sup_{j \geq 1} (k_j |u_j|) \left| \sum_{j=1}^{\infty} (k_{j+1}^n u_{j+1}^*) (k_{j+2}^n u_{j+2}) \right| \quad (47)$$

$$\leq |a| \lambda^{-3n+1} H_n \sup_{j \geq 1} (k_j |u_j|) , \quad (48)$$

where we have used $k_j^n = \lambda^{-np} k_{j+p}^n$ and the Cauchy–Schwarz inequality. The terms with coefficients b and $c = -(a+b)$ are treated in a similar manner. The first ladder inequality is thus proved by using (46) and the estimates for the nonlinear terms in (45).

To prove (43b), we start again from (45). The forcing term is estimated as above. The term with coefficient a is now manipulated as follows :

$$\left| a \sum_{j=1}^{\infty} k_j^{2n} k_{j+1} u_j^* u_{j+1}^* u_{j+2} \right| \leq |a| \lambda \sup_{j \geq 1} |u_j| \left| \sum_{j=1}^{\infty} (k_j^n u_{j+1}^*) (k_j^{n+1} u_{j+2}) \right| \quad (49)$$

$$\leq |a| \lambda^{-3n-1} H_n^{\frac{1}{2}} H_{n+1}^{\frac{1}{2}} \sup_{j \geq 1} |u_j| , \quad (50)$$

where we have used the Cauchy–Schwarz inequality. We then estimate the terms with coefficient b and c in a similar way and use Young’s inequality to find

$$\left| \sum_{j=1}^{\infty} k_j^{2n} u_j^* [(ak_{j+1}u_{j+1}^*u_{j+2} + bk_ju_{j+1}u_{j-1}^* - ck_{j-1}u_{j-1}u_{j-2}) + \text{c.c.}] \right| \quad (51)$$

$$\leq 2\sqrt{2d_n} H_n^{\frac{1}{2}} H_{n+1}^{\frac{1}{2}} \sup_{j \geq 1} |u_j| \leq \nu H_{n+1} + \frac{2d_n}{\nu} H_n \sup_{j \geq 1} |u_j|^2 , \quad (52)$$

where d_n is defined in (44). Finally, we combine the first term on the right-hand side of (52) with the viscous term in (45) and add the estimate of the forcing term to get (43b). \square

The structure of the ladder inequalities makes it evident that control over a low- n rung of the ladder automatically yields control over all the higher-order rungs [34, 35]. Since $\sup_{j \geq 1} |u_j|^2 \leq H_0$ and H_0 is bounded [25], inequality (61b) can be used to prove that there are absorbing balls for all the H_n . The existence of absorbing balls was proved in [25] by using different methods. Here we show how this result follows immediately

from the ladder inequalities and, in addition, we estimate the radius of the absorbing ball for H_n under the assumption that Φ_n is finite.

Corollary 1. *Let $n \geq 0$ and assume the forcing is such that $\Phi_n < \infty$, then*

$$\limsup_{t \rightarrow \infty} H_n \leq \nu^2 k_f^{2(n+1)} \left[\tilde{d}_n \rho^{4(n+1)} Gr^{2(n+1)} + \tilde{C}_n \rho^{\frac{8}{n+2}} Gr^2 \right], \quad (53)$$

where $\rho = k_f/k_1$ and

$$\tilde{d}_n = 2^n d_n^n, \quad \tilde{C}_n = 2^{\frac{2n}{n+2}} C_n^{\frac{n}{n+2}}. \quad (54)$$

Proof. By using $\sup_{j \geq 1} |u_j|^2 \leq H_0$ and the inequality (see the Appendix for the proof)

$$H_n \leq H_0^{\frac{1}{n+1}} H_{n+1}^{\frac{n}{n+1}}, \quad (55)$$

we rewrite (61b) as

$$\dot{H}_n \leq -H_n \left[\nu \frac{H_n^{\frac{1}{n}}}{H_0^{\frac{1}{n}}} - \frac{2d_n}{\nu} H_0 - 2 \frac{\Phi_n^{\frac{1}{2}}}{H_n^{\frac{1}{2}}} \right]. \quad (56)$$

It follows that

$$\limsup_{t \rightarrow \infty} H_n \leq 2^n d_n^n \nu^{-2n} \limsup_{t \rightarrow \infty} H_0^{n+1} + 2^{\frac{2n}{n+2}} \nu^{-\frac{2n}{n+2}} \Phi_n^{\frac{n}{n+2}} \limsup_{t \rightarrow \infty} H_0^{\frac{2}{n+2}}. \quad (57)$$

From Lemma 1, we have

$$\Phi_n = C_n k_f^{2n} |\mathcal{F}|^2 = C_n \nu^4 k_f^{2n+6} Gr^2. \quad (58)$$

In addition, it was shown in [25] that

$$\limsup_{t \rightarrow \infty} H_0 \leq \nu^2 \left(\frac{k_f}{k_1} \right)^4 k_f^2 Gr^2. \quad (59)$$

Inserting (58) and (59) into (57) yields the advertised result. \square

It is also useful to reformulate the ladder inequalities in terms of the quantities

$$K_n = H_n + \tau^2 \Phi_n \quad \text{with} \quad \tau = \nu^{-1} k_0^{-2}, \quad (60)$$

which incorporate the contribution of the forcing. This can be achieved under the additional assumption that the forcing has a cutoff in the spectrum, i.e. there exists a maximum wavenumber $k_{\max} = k_0 \lambda^{j_{\max}}$ such that $f_j = 0$ for $j > j_{\max}$.

Corollary 2. *If $n \geq 0$ and the forcing has a maximum wavenumber k_{\max} and is such that $\Phi_n < \infty$, then K_n satisfies*

$$\frac{1}{2} \dot{K}_n \leq -\nu K_{n+1} + c_n K_n \sup_{j \geq 1} k_j |u_j| + \nu (k_0^2 + k_{\max}^2) K_n \quad (61a)$$

and

$$\frac{1}{2} \dot{K}_n \leq -\frac{\nu}{2} K_{n+1} + \frac{d_n}{\nu} K_n \sup_{j \geq 1} |u_j|^2 + \nu (k_0^2 + k_{\max}^2) K_n. \quad (61b)$$

Proof. The strategy for deriving (43a) from (61a) is the same as for the NSEs [7, 35]. Note first that $\dot{H}_n = \dot{K}_n$. Then, add and subtract $\nu\tau^2\Phi_{n+1}$ to the right-hand side of (43a) to obtain the negative definite term in (61a). The remaining two terms of the H_n inequality are expressed in terms of K_n via the obvious bounds $H_n \leq K_n$ and $\Phi_n \leq \tau^{-2}K_n$. Finally, we are left with the term $\nu\tau^2\Phi_{n+1}$, which is estimated by using $\tau^2\Phi_{n+1} \leq \Phi_{n+1}K_n/\Phi_n \leq k_{\max}^2 K_n$.

Inequality (61b) is proved in exactly the same manner. \square

4.2. A bound for the time average $\left\langle H_n^{\frac{2}{n+1}} \right\rangle_T$

We now make use of the first ladder inequality and the estimate for ϵ to prove the shell-model analogue of a Navier–Stokes result of Foias, Guillopé and Temam [38]. It ought to be noted that the exponent of H_n in the bound below is greater than that found for the 3D NSEs. The reason for this difference between the shell model and the 3D NSEs is discussed in Sect. 5.

Theorem 3. *Let $n \geq 1$ and $E(0) < \infty$ and assume that the forcing (f_1, f_2, \dots) has a maximum wavenumber k_{\max} and is such that $\Phi_n < \infty$. Then, for $Re \gg 1$,*

$$\left\langle H_n^{\frac{2}{n+1}} \right\rangle_T \leq \hat{c}_n \nu^{\frac{4}{n+1}} k_f^4 Re^3 + O(T^{-1}), \quad (62)$$

where the dimensionless positive constant \hat{c}_n depends on a, b, λ, n but is uniform in $\nu, k_0, k_f, k_{\max}, |\mathcal{F}|$.

Proof. By noting that

$$\sup_{j \geq 1} k_j |u_j| = \left(\sup_{j \geq 1} k_j^2 |u_j|^2 \right)^{1/2} \leq H_1^{1/2}, \quad (63)$$

we turn (61a) into

$$\frac{1}{2} \dot{K}_n \leq -\nu K_{n+1} + c_n \widehat{H}_1^{1/2} K_n, \quad (64)$$

where we have denoted $\widehat{H}_1^{1/2} = H_1^{1/2} + 2\nu k_{\max}^2$ and have used $k_0 < k_{\max}$. We shall see that the additive constant in $\widehat{H}_1^{1/2}$ gives a negligible contribution at large Re .

We then divide (64) by $K_n^{\frac{n}{n+1}}$ and time average. The time-derivative term can be simplified as follows:

$$\left\langle K_n^{-\frac{n}{n+1}} \dot{K}_n \right\rangle_T = (n+1) \left\langle \frac{d}{dt} K_n^{\frac{1}{n+1}} \right\rangle_T = \frac{n+1}{T} \left[K_n^{\frac{1}{n+1}}(T) - K_n^{\frac{1}{n+1}}(0) \right]. \quad (65)$$

The first term on the right-hand side is bounded below by $(n+1)(\tau^2\Phi_n)^{\frac{1}{n+1}}/T > 0$, while the second one is $O(T^{-1})$. We are therefore left with

$$\left\langle \frac{K_{n+1}}{K_n^{\frac{n}{n+1}}} \right\rangle_T \leq \frac{c_n}{\nu} \left\langle K_n^{\frac{1}{n+1}} \widehat{H}_1^{\frac{1}{2}} \right\rangle_T + O(T^{-1}) \leq \frac{c_n}{\nu} \left\langle K_n^{\frac{2}{n+1}} \right\rangle_T^{\frac{1}{2}} \left\langle \widehat{H}_1 \right\rangle_T^{\frac{1}{2}} + O(T^{-1}). \quad (66)$$

We now estimate the time average of $K_{n+1}^{\frac{2}{n+2}}$ by using (66) and Hölder’s inequality :

$$\left\langle K_{n+1}^{\frac{2}{n+2}} \right\rangle_T = \left\langle \left(\frac{K_{n+1}}{K_n^{\frac{n}{n+1}}} \right)^{\frac{2}{n+2}} K_n^{\frac{2n}{(n+1)(n+2)}} \right\rangle_T \leq \left\langle \frac{K_{n+1}}{K_n^{\frac{n}{n+1}}} \right\rangle_T^{\frac{2}{n+2}} \left\langle K_n^{\frac{2}{n+2}} \right\rangle_T^{\frac{n}{n+2}} \quad (67)$$

$$\leq c'_n \nu^{-\frac{2}{n+2}} \left\langle K_n^{\frac{2}{n+2}} \right\rangle_T^{\frac{n+1}{n+2}} \left\langle \widehat{H}_1 \right\rangle_T^{\frac{1}{n+2}} + O(T^{-1}) \quad (68)$$

with $c'_n = c_n^{\frac{2}{n+2}}$. Define now the dimensionless quantities

$$A_1 = \nu^{-2} k_f^{-4} \left\langle \widehat{H}_1 \right\rangle_T \quad \text{and} \quad A_n = \nu^{-\frac{4}{n+1}} k_f^{-4} \left\langle K_n^{\frac{2}{n+1}} \right\rangle_T \quad (69)$$

for $n \geq 2$. The bound in (68) then takes the form

$$\langle A_{n+1} \rangle_T \leq c'_n \langle A_n \rangle_T^{\frac{n+1}{n+2}} \langle A_1 \rangle_T^{\frac{1}{n+2}} + O(T^{-1}) \quad (70)$$

and, after the use of Young’s inequality,

$$\langle A_{n+1} \rangle_T \leq \frac{c'_n(n+1)}{n+2} \langle A_n \rangle_T + \frac{c'_n}{n+2} \langle A_1 \rangle_T + O(T^{-1}) . \quad (71)$$

To estimate A_1 , we invoke Jensen’s inequality, (41), and Theorem 1 for $Re \gg 1$:

$$\langle A_1 \rangle_T \leq \nu^{-2} k_f^{-4} \langle H_1 \rangle_T + 4\nu^{-1} k_f^{-4} k_{\max}^2 \langle H_1 \rangle_T^{1/2} + 4k_f^{-4} k_{\max}^4 \leq \hat{c}_1 Re^3 + O(T^{-1}) . \quad (72)$$

Here \hat{c}_1 is a dimensionless constant that depends on a , b , λ and is uniform in ν , k_0 , k_f , k_{\max} , $|\mathcal{F}|$. We now use (72) in (71) for $n = 1$ to estimate $\langle A_2 \rangle_T$ and then proceed iteratively to find

$$\langle A_n \rangle_T \leq \hat{c}_n Re^3 + O(T^{-1}) . \quad (73)$$

We obtain the final result by writing the latter bound in dimensional form and recalling that $H_n \leq K_n$. \square

4.3. High-order moments of the velocity derivatives

For Navier–Stokes flows, the deviations of the velocity and its derivatives from their mean values are captured by the norms $\|\nabla^n \mathbf{u}\|_{L^{2m}}$, where $0 \leq n$ and $1 \leq m \leq \infty$ [10]. For $m < \infty$, the shell-model analogues of $\|\nabla^n \mathbf{u}\|_{L^{2m}}^{2m}$ are

$$H_{n,m} = \sum_{j=1}^{\infty} k_j^{2nm} |u_j|^{2m} , \quad (74)$$

which reduce to H_n when $m = 1$. Instead, the analogue of $\|\nabla^n \mathbf{u}\|_{L^\infty}$ is $\sup_{j \geq 1} k_j^n |u_j|$.

By building on the results of the previous sections, we can generalize Theorem 3 to $H_{n,m}$. Note once again that the exponent of $H_{n,m}$ in the time average differs from that found for weak solutions of the 3D NSEs [10].

Theorem 4. *Under the same assumptions as in Theorem 3 and for $Re \gg 1$, $H_{n,m}$ satisfies*

$$\left\langle H_{n,m}^{\frac{2}{m(n+1)}} \right\rangle_T \leq \hat{c}_n \nu^{\frac{4}{n+1}} k_f^4 Re^3 + O(T^{-1}) \quad (75)$$

if $1 \leq n$, $1 \leq m < \infty$, and

$$\left\langle H_{0,m}^{\frac{1}{m}} \right\rangle_T \leq \nu^2 k_f^2 Re^2 \quad (76)$$

if $n = 0$ and $1 \leq m < \infty$. In addition, for $n \geq 1$

$$\left\langle \left(\sup_{j \geq 1} k_j^n |u_j| \right)^{\frac{4}{n+1}} \right\rangle_T \leq \hat{c}_n \nu^{\frac{4}{n+1}} k_f^4 Re^3 + O(T^{-1}), \quad (77)$$

while for $n = 0$

$$\left\langle \left(\sup_{j \geq 1} |u_j| \right)^2 \right\rangle_T \leq \nu^2 k_f^2 Re^2. \quad (78)$$

The constants \hat{c}_n depend on a, b, λ, n , but are uniform in $\nu, k_0, k_f, k_{\max}, |\mathcal{F}|$.

Proof. The case $m = 1$ was proved in Theorem 3. For $1 < m < \infty$, we use the inequality

$$\sum_{j=1}^{\infty} X_j \leq \left(\sum_{j=1}^{\infty} X_j^{1/p} \right)^p, \quad (79)$$

where $p \geq 1$ and $X_j \geq 0$ for all j . When applied to $H_{n,m}$, this inequality yields

$$H_{n,m} \leq H_n^m. \quad (80)$$

If $n \geq 1$, the result follows from raising both sides of (80) to the power $2/m(n+1)$ and invoking Theorem 3. For $n = 0$, it is proved by raising both sides of (80) to the power $1/m$ and using $H_0 = \nu^2 k_f^2 Re$.

Finally, (77) is proved by noting that

$$\left(\sup_{j \geq 1} k_j^n |u_j| \right)^{\frac{4}{n+1}} = \left(\sup_{j \geq 1} k_j^{2n} |u_j|^2 \right)^{\frac{2}{n+1}} \leq H_n^{\frac{2}{n+1}} \quad (81)$$

and using Theorem 3, while (78) follows from $\sup_{j \geq 1} |u_j|^2 \leq H_0$. \square

5. Comparison with the velocity gradient averaged Navier–Stokes equations

The issue in this section concerns how the velocity derivative estimates displayed in Theorem 4 compare with those for the NSEs. It is not clear that there necessarily should be a positive comparison, given that the 3D NSEs are not known to be regular and their corresponding scaling exponents defined in (2) and (4) are different, namely :

$$\alpha_{n,m} = \frac{2m}{2m(n+1) - 3} \quad (\text{NSE}) \quad \alpha_{n,m} = \frac{4}{n+1} \quad (\text{Shell}). \quad (82)$$

As we will now show, the real comparison lies with what we have called the “velocity gradient averaged Navier–Stokes equations” (VGA-NSEs). To explain the origin of this

name, let us return to the first ladder inequality for H_n displayed in (43a), which for the NSEs is written in the form

$$\frac{1}{2}\dot{H}_n \leq -\nu H_{n+1} + c_n \|\nabla \mathbf{u}\|_\infty H_n, \quad (83)$$

where for simplicity, we have ignored the forcing term [34, 35]. As explained in (9) in §1, the approximation where the L^∞ -norm is replaced by its spatial average

$$\|\nabla \mathbf{u}\|_\infty \approx c L^{-3/2} \|\nabla \mathbf{u}\|_2 \quad (84)$$

has the effect of suppressing intermittent events in $\nabla \mathbf{u}$. Thus we are not dealing with a modified PDE but with an averaging of its solutions reflected in the behaviour of $\|\nabla \mathbf{u}\|_\infty$. In terms of the H_n -ladder we are dealing with

$$\frac{1}{2}\dot{H}_n \leq -\nu H_{n+1} + c_n L^{-3/2} \|\nabla \mathbf{u}\|_2 H_n \quad (85)$$

which yields the exact equivalent of Theorem 3:

Theorem 5. *For $n \geq 1$, the H_n for the 3D VGA-NSEs obey the bounds*

$$\left\langle H_n^{\frac{2}{n+1}} \right\rangle_T \leq c_n L^{-\frac{2(2n-1)}{n+1}} \nu^{\frac{4}{n+1}} Re^3. \quad (86)$$

Remark 2. *Bounds for $H_{n,m}$ follow in the same manner as in Theorem 4, as can be easily seen by using approximation (10) in the proof of Theorem 1 of [9]. The relaxation of the L^∞ to the L^2 -norm in (10) accounts for the insensitivity of the exponents to the value of m .*

Proof. To mimic the FGT-analysis of Theorem 3, and suppressing the multiplicative factors of L and ν , we divide (85) by $H_n^{\frac{n}{n+1}}$ to obtain

$$\begin{aligned} \left\langle \frac{H_{n+1}}{H_n^{\frac{n}{n+1}}} \right\rangle_T &\leq \left\langle H_1^{1/2} H_n^{\frac{1}{n+1}} \right\rangle_T \\ &\leq \langle H_1 \rangle_T^{1/2} \left\langle H_n^{\frac{2}{n+1}} \right\rangle_T^{1/2} \end{aligned} \quad (87)$$

Moreover,

$$\begin{aligned} \left\langle H_n^{\frac{2}{n+2}} \right\rangle_T &= \left\langle \left(\frac{H_{n+1}}{H_n^{\frac{n}{n+1}}} \right)^{\frac{2}{n+2}} H_n^{\frac{2n}{(n+1)(n+2)}} \right\rangle_T \\ &\leq \left\langle \frac{H_{n+1}}{H_n^{\frac{n}{n+1}}} \right\rangle_T^{\frac{2}{n+2}} \left\langle H_n^{\frac{2}{n+1}} \right\rangle_T^{\frac{n}{n+2}} \end{aligned} \quad (88)$$

Let

$$X_n = \left\langle H_n^{\frac{2}{n+1}} \right\rangle_T \quad (89)$$

|| In this section, c_n is a generic positive constant dependent on n .

then from (88) and (87) we have

$$\begin{aligned}
X_{n+1} &\leq \frac{2}{n+2} \left\langle \frac{H_{n+1}}{H_n^{\frac{n}{n+1}}} \right\rangle_T + \frac{n}{n+2} X_n \\
&\leq \frac{1}{n+2} (\langle H_1 \rangle_T + X_n) + \frac{n}{n+2} X_n \\
&= \frac{1}{n+2} \langle H_1 \rangle_T + \frac{n+1}{n+2} X_n
\end{aligned} \tag{90}$$

Since $X_1 = \langle H_1 \rangle_T \leq Re^3$ we have estimates for every $n \geq 1$ in the form of (86). \square

Theorem 5 holds for $n \geq 1$. What of the velocity field represented by $n = 0$?

Lemma 2. *For $1 \leq m \leq \infty$, the velocity field for the 3D VGA-NSEs obey the bounds*

$$\langle \|\mathbf{u}\|_{2m}^2 \rangle_T \leq c_m \nu^2 L^{-\frac{2m-3}{m}} Re^3. \tag{91}$$

Proof. The Poincaré inequality yields

$$\|\mathbf{u}\|_{2m} \leq c_m L \|\nabla \mathbf{u}\|_{2m} \leq c_m L^{\frac{2m+3}{2m}} \|\nabla \mathbf{u}\|_\infty. \tag{92}$$

Then the $L^\infty \rightarrow L^2$ replacement as in (10) gives

$$\|\mathbf{u}\|_{2m} \leq c L^{-\frac{m-3}{2m}} \|\nabla \mathbf{u}\|_2 \quad \text{for } m \geq 1. \tag{93}$$

This is exactly a ‘less intermittent’ form of Sobolev’s inequality which allows some variation in the L^{2m} -norm on the left-hand side instead of L^6 alone, as in its standard form. \square

Comparing (76) with (91) shows that the equivalence between the shell model and the VGA-NSEs only holds at the level of the velocity derivatives. In shell models, the dependence of the velocity field on Re is even weaker than in the VGA-NSEs. Equivalence at the level of the velocity estimates would be obtained by assuming $\|\mathbf{u}\|_\infty \approx c L^{-3/2} \|\mathbf{u}\|_2$, which corresponds to a suppression of the large fluctuations of the velocity field.

6. Simulations and concluding remarks

To test the mathematical estimates, we have performed numerical simulations of the Sabra model. The parameters are the typical ones used in studies of 3D turbulence: $a = 1$, $b = c = -1/2$, $k_0 = 2^{-4}$, $\lambda = 2$ [30]. The forcing has the form $f_j = \mathcal{F} \delta_{j,1}$ with $\mathcal{F} = 5 \times 10^{-3}(1 + i)$, and the viscosity is varied between $\nu = 10^{-7}$ and $\nu \approx 6 \times 10^2$. We truncate the system to N shells by imposing the additional boundary conditions $u_{N+1} = u_{N+2} = 0$, where N is varied between 8 and 27 depending on the value of ν . The numerical integration uses a second-order slaved Adams–Bashforth scheme [45] with time step $dt = 10^{-4}$.

Figures 1 to 3 show ϵ , Gr , and $\left\langle H_{n,m}^{\frac{2}{m(n+1)}} \right\rangle_T$ for different values of n and m as a function of Re . The values of Re vary from the ‘laminar’ regime, in which the shell

Definition	Estimate	Reference
$\epsilon = \nu \left\langle \sum_{j=1}^{\infty} k_j^2 u_j ^2 \right\rangle_T$	$\epsilon \leq \nu^3 k_f^4 (c_1 Re^2 + c_2 Re^3)$	(26)
	$\epsilon U^{-3} k_f^{-1} \leq c_1 Re^{-1} + c_2$	(36)
$Gr = \mathcal{F} / \nu^2 k_f^3$	$Gr \leq c'_1 Re + c'_2 Re^2$	(39)
$H_n = \sum_{j=1}^{\infty} k_j^{2n} u_j ^2$	$\left\langle H_n^{\frac{2}{n+1}} \right\rangle_T \leq \hat{c}_n \nu^{\frac{4}{n+1}} k_f^4 Re^3 \quad (n \geq 1, Re \gg 1)$	(62)
$H_{n,m} = \sum_{j=1}^{\infty} k_j^{2nm} u_j ^{2m}$	$\left\langle H_{n,m}^{\frac{2}{m(n+1)}} \right\rangle_T \leq \hat{c}_n \nu^{\frac{4}{m(n+1)}} k_f^4 Re^3 \quad (n \geq 1, Re \gg 1)$	(75)
$H_{0,m} = \sum_{j=1}^{\infty} u_j ^{2m}$	$\left\langle H_{0,m}^{1/m} \right\rangle_T \leq \nu^2 k_f^2 Re^2$	(76)
	$\left\langle \left(\sup_{j \geq 1} k_j^n u_j \right)^{\frac{4}{n+1}} \right\rangle_T \leq \hat{c}_n \nu^{\frac{4}{n+1}} k_f^4 Re^3 \quad (n \geq 1)$	(77)
	$\left\langle \left(\sup_{j \geq 1} u_j \right)^2 \right\rangle_T \leq \nu^2 k_f^2 Re^2$	(78)

Table 1. Summary of the main estimates and definitions for the shell model. The $O(T^{-1})$ corrections have not been included for simplicity.

model relaxes to a fixed point, to the fully turbulent regime, which is characterized by a $k_j^{-5/3}$ spectrum over several decades of wavenumbers. To facilitate the reading of the figures, the relevant definitions and estimates for shell models are summarized in Table 1. The shell-model estimates are then compared with those for the 3D NSEs and VGA NSEs in Table 2.

The simulations clearly show that the mathematical estimates in Table 1 accurately describe the behaviour of the shell model as a function of Re . Figure 2(b) also indicate that, for $Re \ll 1$, the scaling of $\left\langle H_n^{\frac{2}{n+1}} \right\rangle_T$ depends on n , as may be inferred from the proof of Theorem 3 (see (70) to (72)). Related to this, in Fig. 3(a) the small- Re scaling of $\left\langle H_{n,m}^{\frac{2}{m(n+1)}} \right\rangle_T$ depends on n but not on m , as a consequence of $H_{n,m}$ being controlled by H_n^m (see (80)).

Our conclusion is that shell models behave more closely to the 3D VGA-NSEs than the NSEs themselves. They both have identical scaling exponents in their time averages of their velocity derivatives which are reflected in the suppression of strong events of $\nabla \mathbf{u}$, as proposed in equation (10). The actual properties of shell models for the velocity field itself are even milder than the estimates for the VGA-NSEs: compare (76) in Table 1 with (91).

Finally, we ask how much more regularity do solutions of shell models possess

	3D NSEs	3D VGA NSEs	Shell model
$F_{n,m}$	$\nu^{-1} L^{\frac{2m(n+1)-3}{2m}} \ \nabla^n \mathbf{u}\ _{2m}$	$\nu^{-1} L^{\frac{2m(n+1)-3}{2m}} \ \nabla^n \mathbf{u}\ _{2m}$	$\nu^{-1} k_f^{-n-1} \left(\sum_{j=1}^{\infty} k_j^{2nm} u_j ^{2m} \right)^{\frac{1}{2m}}$
$\alpha_{n,m}$	$\frac{2m}{2m(n+1)-3}$	$\frac{4}{n+1}$	$\frac{4}{n+1}$
$1 \leq n, 1 \leq m \leq \infty$	$\langle F_{n,m}^{\alpha_{n,m}} \rangle_T \leq c_{n,m} Re^3$	$\langle F_{n,m}^{\alpha_{n,m}} \rangle_T \leq c_{n,m} Re^3$	$\langle F_{n,m}^{\alpha_{n,m}} \rangle_T \leq \hat{c}_n Re^3$
$n = 0, 1 \leq m \leq \infty$	$\langle F_{0,m}^{\alpha_{0,m}} \rangle_T \leq c_{0,m} Re^3$ (only for $3 < m \leq \infty$)	$\langle F_{0,m}^2 \rangle_T \leq c_m Re^3$	$\langle F_{0,m}^2 \rangle_T \leq Re^2$

Table 2. Comparison of the estimates for the 3D NSEs, the 3D VGA NSEs, and the shell model. In the above estimates, $Re \gg 1$ and the $O(T^{-1})$ corrections have not been included for simplicity.

than those for the NSEs? This is shown up by comparing the estimates for velocity derivatives. Consider the scaling exponents $\alpha_{n,m}$ defined in (3) which appear in (4). It is not difficult to replicate this result in $D = 3, 2, 1$ dimensions [10]. $\alpha_{n,m}$ is replaced by $\alpha_{n,m,D}$

$$\alpha_{n,m,D} = \frac{2m}{2m(n+1) - D} \quad (94)$$

and the relation involving $F_{n,m}$ in (4) is replaced by

$$\left\langle F_{n,m,D}^{(4-D)\alpha_{n,m,D}} \right\rangle_T \leq c_{n,m,D} Re^3. \quad (95)$$

In all these estimates, the larger the exponent the more regularity we have. Under what conditions is the $4/(n+1)$ of shell models greater than $(4-D)\alpha_{n,m,D}$?

$$\frac{4}{n+1} \geq (4-D)\alpha_{n,m,D} ? \quad (96)$$

The answer turns out to be

$$2D \{m(n+1) - 2\} \geq 0, \quad (97)$$

and is thus always true when $n \geq 1$ and $m \geq 1$ for every value of D . Equality holds only at the level of the energy dissipation rate when $n = m = 1$. The same result implies that, exception made for the time-averaged dissipation rate, the Re -dependence of the velocity derivatives is weaker for shell models than for the D -dimensional NSEs for any integer D . Curiously, in a formal manner, equality also holds in the limit $D \rightarrow 0$, which corresponds to the ‘‘Navier–Stokes equations on a point’’, which has zero dimension. Since shell models can be regarded as field problems in zero spatial dimension [46], the physical correspondence between the two is intriguing.

We conclude by discussing possible extensions of this work. To our knowledge, the mathematical estimates for the 3D NSEs have been compared with numerical simulations of turbulent flows only for $n = 1$ [15]. In order further to study the correspondence between shell models and the 3D NSEs, it would be interesting to examine the higher-order derivatives of the velocity field in turbulence simulations.

In shell models, the nonlinear interactions are drastically truncated to few Fourier modes. There exist various extensions of shell models aimed at better approximating the structure of the NSEs in Fourier space, for instance dyadic models on trees [46,47]. These refined models may show a behaviour closer to that of the 3D NSEs, but the solution remains an element of a sequence space, and hence its infinity norm is dominated by all norms of finite order. Such a property has been identified as the main reason for the weaker dependence on Re in shell models. It is therefore expected that a similar behaviour will be found in dyadic models on trees.

While the regularity problem remains unsolved for the 3D NSEs, it was shown in Ref. [48] that suitably ‘decimating’ the Fourier modes of the velocity field so as to project the NSEs onto a subspace with sign-definite helicity induces regularity. It would be worth exploring whether the regularity of the helically-decimated NSEs leads to a close correspondence with their shell-model counterpart.

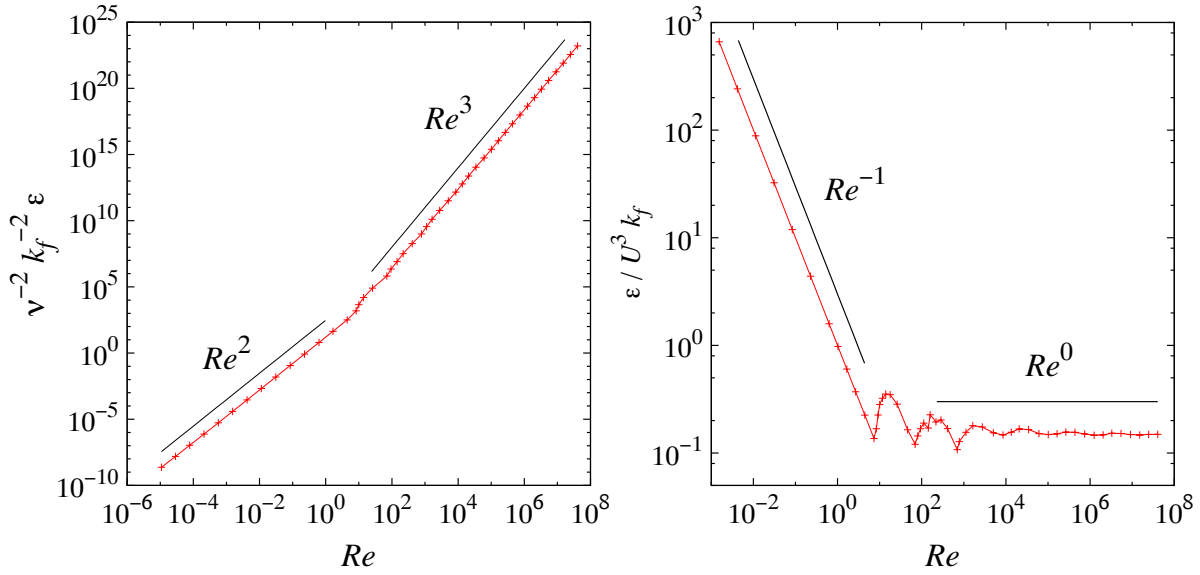


Figure 1. Rescaled time-averaged energy dissipation rate as a function of the Reynolds number.

Finally, it was recalled in the introduction that the moments of the derivatives of a turbulent velocity field can be estimated by using the multifractal formalism. It ought to be noted that the quantities examined here differ from those commonly considered within the multifractal formalism, which studies estimates of the form $\langle \|\nabla^n \mathbf{u}\|_{2m}^{2m} \rangle_T \sim Re^{\rho_{n,m}}$ [1, 11, 12]. In our estimates (see Table 2), the exponent $\alpha_{n,m}$ is a decreasing function of both n and m and is inserted in between the space and time averages. On the one hand, this has the consequence that the dependence on m and n is entirely contained within the averages of the velocity derivatives rather than appearing in the exponent of the Reynolds number. On the other hand, the quantities considered in our study may be difficult to analyze with the multifractal formalism, which does not distinguish easily between space and time averages. Establishing a connection between the mathematical estimates and the multifractal formalism would contribute greatly to the understanding of the intermittent nature of turbulent flows.

Acknowledgments

The authors are grateful to Samriddhi Sankar Ray for several useful suggestions. John Gibbon acknowledges the award of a Visiting Professorship at the Université Côte d’Azur during the months of November 2018 and April 2019 and the kind hospitality of the Laboratoire J. A. Dieudonné.

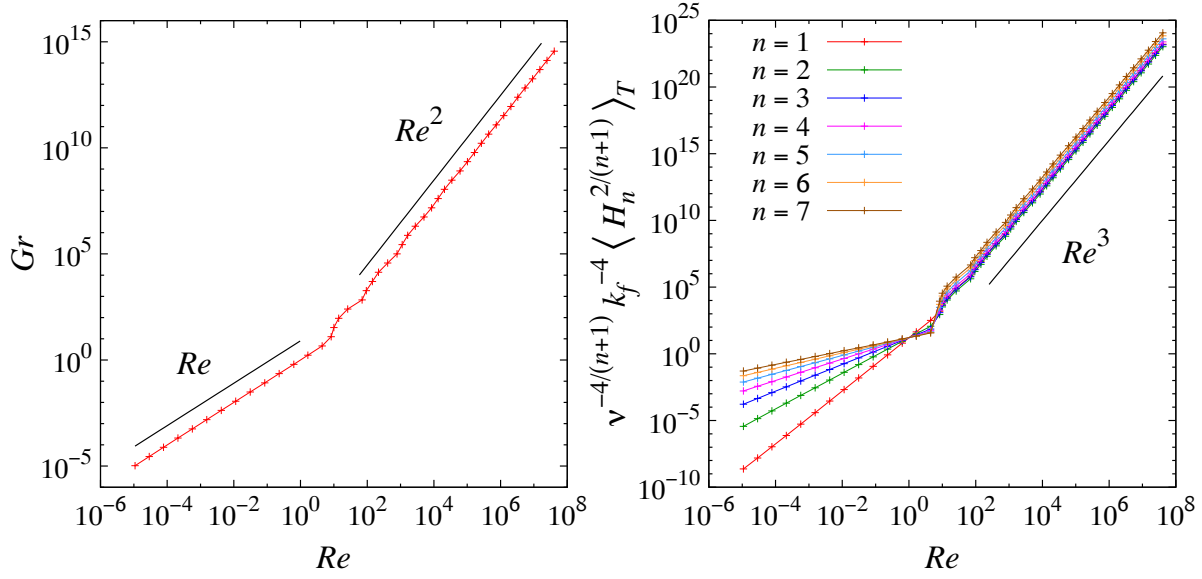


Figure 2. (a) Grashof number as a function of the Reynolds number; (b) Time average of $H_n^{\frac{2}{n+1}}$ rescaled by $\nu^{\frac{4}{n+1}} k_f^4$ as a function of the Reynolds number.

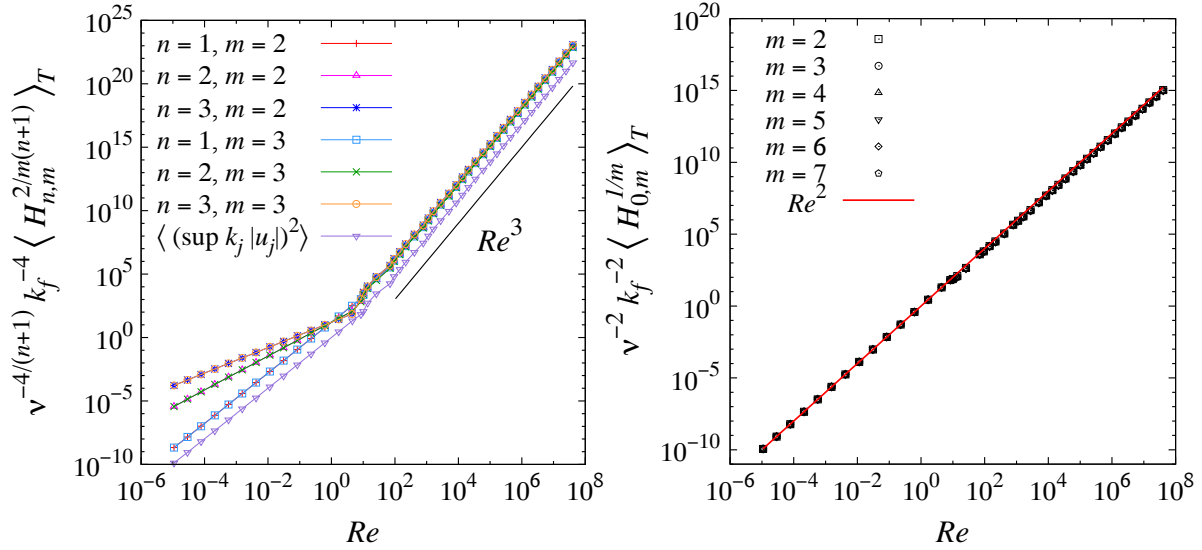


Figure 3. Time averages of (a) $H_{n,m}^{\frac{2}{m(n+1)}}$ rescaled by $\nu^{\frac{4}{n+1}} k_f^4$ and (b) $H_{0,m}^{\frac{1}{m}}$ rescaled by $\nu^2 k_f^2$ as a function of the Reynolds number.

Appendix

Inequality (55) is proved by induction on n [35]. By using the Cauchy–Schwarz inequality, we find

$$H_1 = \sum_{j=1}^{\infty} |u_j| (k_j^2 |u_j|) \leq H_0^{\frac{1}{2}} H_2^{\frac{1}{2}}. \quad (\text{A.1})$$

We then assume

$$H_n \leq H_0^{\frac{1}{n+1}} H_{n+1}^{\frac{n}{n+1}} \quad (\text{A.2})$$

and estimate H_{n+1} as

$$H_{n+1} \leq H_n^{\frac{1}{2}} H_{n+2}^{\frac{1}{2}} \leq H_0^{\frac{1}{2(n+1)}} H_{n+1}^{\frac{n}{2(n+1)}} H_{n+2}^{\frac{1}{2}}, \quad (\text{A.3})$$

which yields

$$H_{n+1} \leq H_0^{\frac{1}{n+2}} H_{n+2}^{\frac{n+1}{n+2}}. \quad (\text{A.4})$$

This completes the proof by induction.

References

- [1] Frisch U 1995 *Turbulence: The Legacy of A. N. Kolmogorov* (Cambridge, UK: Cambridge University Press)
- [2] Sreenivasan K R and Antonia R A 1997 The phenomenology of small-scale turbulence *Annu. Rev. Fluid Mech.* **29**, 435–472
- [3] Sreenivasan K R 1999 Fluid turbulence *Rev. Mod. Phys.* **71** 383–95
- [4] Davidson P A 2004 *Turbulence: An Introduction for Scientists & Engineers*, (1st ed) Oxford University Press
- [5] Sreenivasan K R 1984 On the scaling of the turbulence energy dissipation rate *Phys. Fluids* **27** 1048–51
- [6] Doering C R 2009 The 3D Navier–Stokes Problem *Annu. Rev. Fluid Mech.* **41** 109–28
- [7] Bartuccelli M V, Doering C R, Gibbon J D and Malham S J A 1993 Length scales in solutions of the Navier–Stokes equations *Nonlinearity* **6** 549–68
- [8] Gibbon J D 2012 A hierarchy of length scales for weak solutions of the three-dimensional Navier–Stokes equations *Commun. Math. Sci.* **10** 131–6
- [9] Gibbon J D 2019 Weak and strong solutions of the 3D Navier–Stokes equations and their relation to a chessboard of convergent inverse length scales *J. Nonlinear Sci.* **29**, 215–28
- [10] Gibbon J D 2020 *Intermittency, cascades and thin sets in three-dimensional Navier-Stokes turbulence* – in preparation.
- [11] Nelkin M 1990 Multifractal scaling of velocity derivatives in turbulence *Phys. Rev. A* **42**, 7226–9
- [12] Benzi R, Biferale L, Paladin G, Vulpiani A and Vergassola M 1991 Multifractality in the statistics of the velocity gradients in turbulence *Phys. Rev. Lett.* **67**, 2299–302
- [13] Schumacher J, Sreenivasan K R and Yakhot V 2007 Asymptotic exponents from low-Reynolds number flows *New J. Phys.* **9**, 89
- [14] Chakraborty S, Frisch U, Pauls W and Ray S S 2012 Nelkin scaling for the Burgers equation and the role of high-precision calculations *Phys. Rev. E* **85**, 015301(R)
- [15] Donzis D, Gibbon J D, Gupta A, Kerr R M, Pandit R and Vincenzi D 2013 Vorticity moments in four numerical simulations of the 3D Navier–Stokes equations *J. Fluid Mech.* **732**, 316–31
- [16] Landau L D and Lifshitz E M 1987 *Fluid Mechanics*, 2nd ed. (Burlington, MA: Butterworth-Heinemann)
- [17] Moin P and Mahesh K 1998 Direct numerical simulation: A tool in turbulence research *Annu. Rev. Fluid Mech.* **30**, 539–78
- [18] Celani A 2007 The frontiers of computing in turbulence: challenges and perspectives *J. Turbul.* **8** N34
- [19] Ishihara T, Gotoh T and Kaneda Y 2009 Study of high-Reynolds number isotropic turbulence by direct numerical simulation *Ann Rev Fluid Mech.* **41** 165–80
- [20] Donzis D, Yeung P K and Sreenivasan K R 2008 Dissipation and enstrophy in isotropic turbulence: Resolution effects and scaling in direct numerical simulations *Phys. Fluids* **20**, 045108
- [21] Kerr R M 2012 Dissipation and enstrophy statistics in turbulence: are the simulations and mathematics converging? *J Fluid Mech.* **700** 1–4

- [22] Bohr T, Jensen M H, Paladin G and Vulpiani A 1998 *Dynamical Systems Approach to Turbulence* (Cambridge, UK: Cambridge University Press)
- [23] Biferale L 2003 Shell models of energy cascade in turbulence *Annu. Rev. Fluid Mech.* **35** 441–68
- [24] Ditlevsen P D 2010 *Turbulence and Shell Models* (Cambridge, UK: Cambridge University Press)
- [25] Constantin P, Levant B and Titi E S 2006 Analytic study of shell models of turbulence *Physica D* **219** 120–41
- [26] Constantin P, Levant B and Titi E S 2007 Sharp lower bounds for the dimension of the global attractor of the Sabra shell model of turbulence *J. Stat. Phys.* **127** 1173–92
- [27] Barbato D, Barsanti M, Bessaih H and Flandoli F 2006 Some rigorous results on a stochastic GOY model *J. Stat. Phys.* **125** 677–716
- [28] L’vov V S, Podivilov E, Pomyalov A, Procaccia I and Vandembroucq D 1998 Improved shell model of turbulence *Phys. Rev. E* **58** 1811–22
- [29] Gledzer E B 1973 System of hydrodynamic type admitting two quadratic integrals of motion *Sov. Phys. Dokl.* **18** 216–217
- [30] Yamada M and Ohkitani K 1987 Lyapunov spectrum of a chaotic model of three-dimensional turbulence *J. Phys. Soc. Japan* **56** 4210–3
- [31] Doering C R and Foias C 2002 Energy dissipation in body-forced turbulence *J. Fluid Mech.* **467** 289–306
- [32] Gibbon J D, Gupta A, Krstulovic G, Pandit R, Politano H, Ponty Y, Pouquet A, Sahoo G, and Stawarz J 2016 Depletion of nonlinearity in magnetohydrodynamic turbulence: Insights from analysis and simulations *Phys. Rev. E* **93** 043104
- [33] Gibbon J D, Gupta A, Pal N and Pandit R 2018 The role of BKM-type theorems in 3D Euler, Navier–Stokes and Cahn–Hilliard–Navier–Stokes analysis *Physica D* **376–377**, 60–8
- [34] Bartuccelli M, Doering C and Gibbon J D 1991 Ladder theorems for the 2D and 3D Navier–Stokes equations on a finite periodic domain *Nonlinearity* **4** 531–42
- [35] Doering C R and Gibbon J D 1995 *Applied Analysis of the Navier–Stokes Equations* (Cambridge, UK: Cambridge University Press)
- [36] Constantin P and Foias C. 1988 *Navier–Stokes Equations* (Chicago USA: Chicago University Press)
- [37] Foias C., Manley O., Rosa R. and Temam R. 2001 *Navier–Stokes Equations and Turbulence* (Cambridge, UK: Cambridge University Press)
- [38] Foias C, Guillopé C and Temam R 1981 New a priori estimates for Navier–Stokes equations in dimension 3 *Comm. Part. Differ. Equat.* **6** 329–59
- [39] Gilbert T, L’vov V S, Pomyalov A and Procaccia I 2002 Inverse cascade regime in shell models of two-dimensional turbulence *Phys. Rev. Lett.* **89** 074501
- [40] Boffetta G, Celani A and Roagna D 2000 Energy dissipation statistics in a shell model of turbulence *Phys. Rev. E* **61** 3234–6
- [41] Mazzi B, Okkels F and Vassilicos J C 2002 A shell-model approach to fractal-induced turbulence *Eur. Phys. J. B* **28** 243–51
- [42] Biferale L, Cencini M, Lanotte A S, Sbragaglia M and Toschi F 2004 Anomalous scaling and universality in hydrodynamic systems with power-law forcing *New J. Phys.* **6** 37
- [43] Doering C R and Gibbon J D 2002 Bounds on moments of the energy spectrum for weak solutions of the three-dimensional Navier–Stokes equations *Physica D* **165** 163–75
- [44] Constantin P 1991 *Remarks on the Navier–Stokes equations* in: Sirovich, L. (ed.) *New Perspectives in Turbulence*, pp. 229–261 (Berlin: Springer).
- [45] Pisarenko D, Biferale L, Courvoisier D, Frisch U and Vergassola M 1993 Further results on multifractality in shell models *Phys. Fluids A* **5** 2533–8
- [46] Benzi R, Biferale L, Trovatore E 1997 Ultrametric structure of multiscale energy correlations in turbulent models *Phys. Rev. Lett.* **79**, 1670–3
- [47] Barbato D, Bianchi L A, Flandoli F, Morandin F 2013 A dyadic model on a tree *J. Math. Phys.* **54**, 021507

- [48] Biferale L, Titi E S 2013 On the global regularity of a helical-decimated version of the 3D Navier–Stokes equations *J. Stat. Phys.* **151**, 1089–98